Impact of Gaze Uncertainty on AOIs in Information Visualisations

Yao Wang*
University of Stuttgart
Stuttgart, Germany
yao.wang@vis.uni-stuttgart.de

Maurice Koch*
University of Stuttgart
Stuttgart, Germany
maurice.koch@visus.uni-stuttgart.de

Mihai Bâce
University of Stuttgart
Stuttgart, Germany
mihai.bace@vis.uni-stuttgart.de

Daniel Weiskopf
University of Stuttgart
Stuttgart, Germany
daniel.weiskopf@visus.uni-stuttgart.de

Andreas Bulling
University of Stuttgart
Stuttgart, Germany
andreas.bulling@vis.uni-stuttgart.de

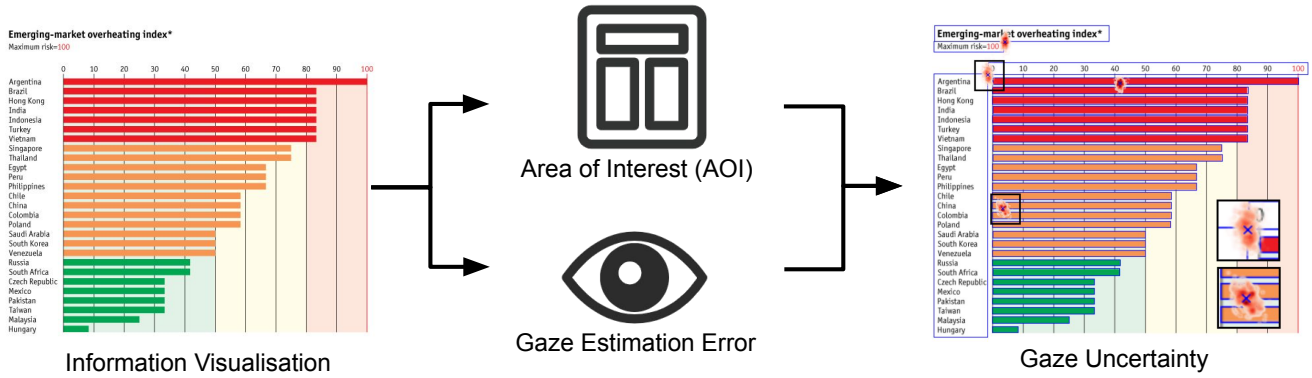

Figure 1: Areas of Interest (AOIs) are used extensively in eye tracking studies, however, it is currently unknown how gaze uncertainty impacts the resulting findings. To overcome this limitation, we study the uncertainty caused by the gaze estimation error of the eye tracker and amplified by the nearby AOIs in information visualisations. We propose two effective metrics, the Flipping Candidate Rate (FCR) and Hit Any AOI Rate (HAAR), to quantify the impact of uncertainty on the sample application domain of information visualisations.

ABSTRACT

Gaze-based analysis of areas of interest (AOIs) is widely used in information visualisation research to understand how people explore visualisations or assess the quality of visualisations concerning key characteristics such as memorability. However, nearby AOIs in visualisations amplify the uncertainty caused by the gaze estimation error, which strongly influences the mapping between gaze samples or fixations and different AOIs. We contribute a novel investigation into gaze uncertainty and quantify its impact on AOI-based analysis on visualisations using two novel metrics: the Flipping Candidate Rate (FCR) and Hit Any AOI Rate (HAAR). Our analysis of 40 real-world visualisations, including human gaze and AOI annotations, shows that gaze uncertainty frequently and significantly impacts the analysis conducted in AOI-based studies. Moreover, we analysed four visualisation types and found that bar and scatter plots are usually designed in a way that causes more uncertainty than line and pie plots in gaze-based analysis.

CCS CONCEPTS

• **Human-centered computing** → **Information visualization**; **Laboratory experiments**.

KEYWORDS

gaze uncertainty, gaze estimation error, eye tracking study, information visualisations

ACM Reference Format:
Yao Wang, Maurice Koch, Mihai Bâce, Daniel Weiskopf, and Andreas Bulling. 2022. Impact of Gaze Uncertainty on AOIs in Information Visualisations. In *2022 Symposium on Eye Tracking Research and Applications (ETRA '22), June 8–11, 2022, Seattle, WA, USA.* ACM, New York, NY, USA, 6 pages. https://doi.org/10.1145/3517031.3531166

1 INTRODUCTION

Gaze-based analysis of different areas of interest (AOIs) is widely used in information visualisation research, e.g. to understand how people explore visualisations [Polatsek et al. 2018] or assess the

*Both authors contributed equally to this research.

ETRA '22, June 8–11, 2022, Seattle, WA, USA
© 2022 Copyright held by the owner/author(s). Publication rights licensed to ACM. This is the author's version of the work. It is posted here for your personal use. Not for redistribution. The definitive Version of Record was published in *2022 Symposium on Eye Tracking Research and Applications (ETRA '22), June 8–11, 2022, Seattle, WA, USA*, https://doi.org/10.1145/3517031.3531166.

quality of information visualisations with respect to memorability [Borkin et al. 2015] or graphic effectiveness [Goldberg and Helfman 2010]. On such visual stimuli, an AOI covers areas with semantic meaning such as the axes, the title, or different graphical elements. However, a key assumption in gaze-based AOI analysis is the correct assignment of gaze samples and fixations to the corresponding AOIs [Goldberg and Helfman 2010]. Despite recent advancements in eye tracking hardware and methods, there is still an inherent gaze estimation error [Ehinger et al. 2019] that causes uncertainty in the on-screen gaze locations. In addition, visualisation characteristics such as the distance between AOIs [Yun et al. 2013] and their sizes [Orquin et al. 2016] further magnify the impact of gaze estimation error on AOI analysis. Several studies have reported this impact on gaze-based applications, e.g. it hampers the conclusion of behavioural decision-making studies [Orquin et al. 2016] and the usability of gaze-based user interfaces [Barz et al. 2016]. To quantify this impact, Orquin and Holmqvist [2018] proposed the capture rate, a statistical metric to quantify the percentage of fixations assigned to a given AOI. The capture rate is dependent on the size of the AOI and the accuracy of the eye tracker. Still, it cannot provide insights into fixations that may belong to multiple AOIs, and is suitable for simpler user interfaces in perceptual studies.

Inspired by previous work on gaze-based AOI analysis, this paper further assesses the impact of gaze uncertainty on the assignment of fixations to AOIs in information visualisations, especially for different visualisation types, such as *line*, *bar*, *scatter*, and *pie plots*. In perception studies [Orquin et al. 2016; Orquin and Holmqvist 2018], researchers can avoid the effect of gaze uncertainty by increasing the AOI sizes and distances between AOIs. However, AOIs in information visualisations are usually small and close to one another. For such stimuli, gaze uncertainty becomes crucial in analysing fixations that land at the borders of possibly multiple AOIs. Moreover, another consequence of gaze uncertainty caused by gaze estimation error could lead to fixations areas with no semantic meaning (e.g. white spaces) and prior research showed that such areas do not attract human attention [Matzen et al. 2017].

In this paper, to quantify gaze uncertainty and its impact on AOI-based analysis for information visualisations, we introduce two novel metrics: the *Flipping Candidate Rate (FCR)* and the *Hit Any AOI Rate (HAAR)*. FCR quantifies the probability that fixations might flip between two or more AOIs. HAAR quantifies the percentage of fixations that land on at least one AOI, hence capturing the impact of gaze uncertainty when assigning fixations to AOIs. To further understand and assess the impact of gaze uncertainty when assigning fixations to AOIs, we artificially flipped assigned AOIs and compared the resulting scanpaths. We calculated the Sequence Score [Yang et al. 2020], which is a pairwise string similarity metric, between the original and altered scanpaths. A value lower than 1 for the sequence score means that the altered scanpaths are different from the original one due to different assignments of fixations to AOIs, which could lead to potentially very different conclusions based on the eye tracking study. The results of our analysis suggest that gaze uncertainty has a substantial influence on AOI-based evaluations, and *bar* and *scatter plots* are most commonly designed in a way that causes more uncertainty than *line* and *pie plots* in gaze-based analysis. The contribution of our work is two-fold: First, we analyse and demonstrate the impact of gaze uncertainty on the assignment of fixations to AOIs for 40 real-world information visualisations [Borkin et al. 2013]. Second, we propose two novel metrics, the FCR and HAAR, that quantify the impact of gaze uncertainty on AOIs.

2 RELATED WORK

Our work is grounded on 1) gaze-based area of interest (AOI) evaluations of information visualisations and 2) gaze estimation error, and it is positioned in the area of 3) uncertainty representation and visualisation. Below, we briefly survey the literature in these fields.

Gaze-based Area of Interest Evaluation. Gaze-based AOI evaluation is widely used for various kinds of visualisations, including web pages [Drusch et al. 2014], static visualisations [Borkin et al. 2015], and metro maps [Xie et al. 2021]. In general, it plays an important role in connecting eye tracking and visualisation research [Burch et al. 2017]. An overview of AOI-oriented data visualization is provided by Blascheck et al. [2017]. The impact of AOI sizes on decision-making studies was examined by Orquin et al. [2016], and capture rate was proposed to quantify the uncertainty about the amount of fixations to a given object [Orquin and Holmqvist 2018].

Gaze Estimation Error. The intrinsic gaze estimation error from eye-tracking devices is well studied [Ehinger et al. 2019; Orquin et al. 2016]. Zhang and Hornof [2014] focused on post-hoc error compensation, whereas Sattar et al. [2017] added "jitter" to gaze samples to simulate different eye trackers. For user interfaces, the implications of the accuracy of eye tracking for design was studied by Feit et al. [2017]. Error-aware gaze-based interfaces allow us to compensate the gaze estimation error [Barz et al. 2016, 2018]. Furthermore, there are filtering and visual-interactive cleansing methods to address data quality problems in eye tracking [Schulz et al. 2015].

Uncertainty Representation and Visualisation. Dealing with uncertainty for gaze and corresponding AOI assignments, we can relate our work to the general problem of representing and processing uncertainty. Skeels et al. [2010] provide a general discussion of different notions of uncertainty and their role in data visualisation. According to their terminology, gaze estimation error can be understood as uncertainty on level 1 (for measurement precision and similar); however, the derived AOI assignment and follow-up analysis can be seen as uncertainty on level 3 — the inference level. Uncertainty visualisation can then use uncertainty models to represent and analyse uncertainty. See, for example, the seminal work by Pang et al. [1997] and a most recent survey on the topic [Weiskopf 2022].

Previous literature either directly used fixations and saccades for further analysis, or mitigated the impact of gaze uncertainty by changing the stimuli. Given AOIs in information visualisations are close and small, a slight change of gaze position might substantially affect the mapping to AOIs. Thus, a fundamental investigation into the impact of gaze estimation error in information visualisations is necessary.

3 GAZE UNCERTAINTY ASSESSMENT

The impact of gaze uncertainty on AOI assignment is assessed from two perspectives: 1) the number of fixation candidates that might flip between AOIs (FCR) and 2) the number of fixations that hit any AOI (HAAR). Both a high FCR and a low HAAR suggest a high level of gaze uncertainty. We conducted our assessment on VisRecall [Wang et al. 2021], a dataset consisting of hundreds of real-world visualisations from MASSVIS [Borkin et al. 2015, 2013], along with human gaze and AOI annotations. The AOIs are annotated following the taxonomy by Borkin et al. [2015]. Gaze data from VisRecall were collected under a recallability task, which includes an encoding and a recalling phase. An EyeLink 1000 Plus eye tracker at 2 kHz was mounted on a 24.5" monitor with a resolution of 1920 × 1080 px. Visualisations were scaled to fit around 21.1 × 14.8° of visual angle in the centre. For our assessment, only the gaze data from the encoding phase are used. We randomly selected 10 visualisations from each visualisation type: *bar*, *pie*, *line*, and *scatter plots*.

3.1 AOI Flipping Candidates

As the first step, we determine the spatial uncertainty associated with fixations. To this end, we take the raw gaze samples within each fixation segment (i.e., the time span associated with a fixation), and apply kernel density estimation (KDE) to arrive at the gaze density distribution [Rayner 1998]. The extent of the estimation error for the input gaze points is controlled by the bandwidth h of a Gaussian kernel K_h. We compute the overlaid gaze density by summing up the contributions from the gaze samples, resulting in the probability density for this fixation.

Our goal is the probability p_i that describes the probability of assigning a fixation to the ith AOI. Therefore, in the second step, p_i is obtained by integrating (i.e., summing over an area) densities over all points that are covered by the i^{th} AOI, that is,

$$p_i = \int_{x \in \Omega} \mathbb{1}_{A_i}(x) \left(\frac{1}{n} \sum_{j=1}^{n} K_h(x - x_j) \right) d^2x$$

Here $x_1, \ldots, x_n$ are the gaze samples associated with the fixation, and $\mathbb{1}_{A_i}(x)$ indicates if the point x in image space Ω is covered by the i^{th} AOI (i.e., $\mathbb{1}_{A_i}(x)$ is the characteristic function for AOI i). Figure 2 illustrates the computation of AOI probabilities.

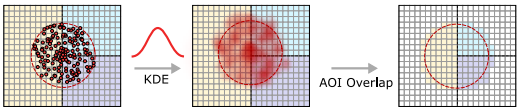

Figure 2: Overview of the basic steps to decide whether a fixation is considered a flipping candidate.

Fixations whose densities only overlay one AOI will have a probability distribution peaked at this AOI, whereas fixations that overlay two or more AOIs to a similar extent will result in distributions that are closer to being uniform over the respective AOIs. We consider the latter type of fixations as flipping candidates. Depending on the number of AOIs that are overlaid by the fixation, we differentiate between different ranks of flipping candidates. For example, Figure 3 illustrates fixations of rank 2 and 3. Given a number of N AOIs, the flipping candidate score s_k of rank k is defined as follows:

$$s_k = \sum_{i=1}^{N} p_i - \left(\sum_{i=1}^{k} \left| p_i - \frac{1}{k} \right| \right)$$

Note that we assume the probabilities p_i to be sorted in descending order, that is, $p_i \geq p_{i+1}$. The first term of the score equation penalises fixations whose spread covers mostly white space and only few AOIs. The second term captures the degree of uncertainty and is defined as the statistical distance between the probabilities p_i and the discrete uniform distribution of length k.

We define a flipping candidate of rank k if its score s_k exceeds a predefined threshold t, and it does not receive higher scores on different ranks, that is, $k = \text{argmax}_j(s_j)$. In this work, we only consider rank $k \in \{2, 3, 4\}$ since it is unlikely that a fixation overlays more than four AOIs. Examples of flipping candidates of rank 2 for *scatter*, *bar*, *line*, and *pie plots* can be found in Figure 4. Here, fixations that receive scores $s_2 > 0.5$ are marked in blue, whereas fixations that receive scores $0 \leq s_2 \leq 0.5$ are marked in orange. As an example, in the pie chart, the fixation located on the pie is marked in blue since its density overlaps with two adjacent data segments to a similar extent. In contrast, the fixation located between the legend and source text is marked in orange since its density mostly covers white space.

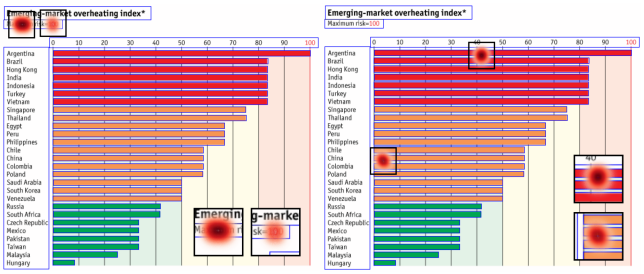

Figure 3: Examples of flipping candidates of rank 2 (left) and rank 3 (right).

3.1.1 Metrics. We propose the Flipping Candidate Rate (FCR) to quantify the probability that fixations might flip between two or more AOIs. Given the above definition of a flipping candidate, we can count the number of flipping candidates occurring in a scanpath and use it as a measure of its uncertainty. Since we intend to compare scanpaths of different lengths, we normalize the number of flipping candidates C by length N to get the FCR = $\frac{C}{N}$ of a scanpath. Therefore, the FCR is a metric that describes how much the gaze estimation error affects the mapping to AOIs.

We then go one step further and measure how much the uncertainty in the AOI mapping impacts later analysis, here for the example of scanpath analysis. To this end, we apply Sequence Score [Yang et al. 2020], a pairwise string similarity metric that is normalized between 0 and 1, where 1 suggests a perfect match. Each fixation in a scanpath is mapped to a character in a string based on its AOI label. We alter all flipping candidates in a scanpath to the second most probable AOI according to the FCR, and compute the Sequence Score between the original and flipped scanpaths.

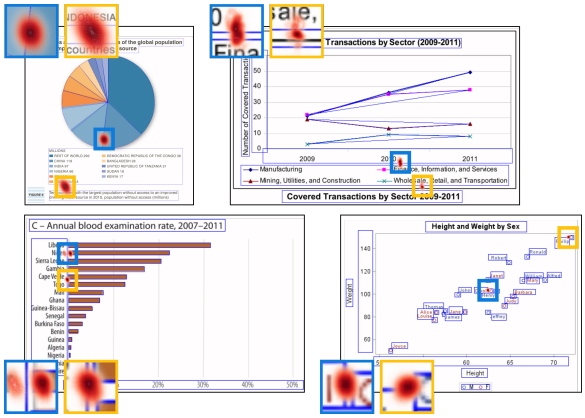

Figure 4: Examples of flipping candidates of rank 2 in pie, line, bar, and scatter plots. Fixations whose flipping candidate score satisfies $0 \leq s_2 \leq 0.5$ are marked in orange, while fixations with $s_2 > 0.5$ are marked in blue.

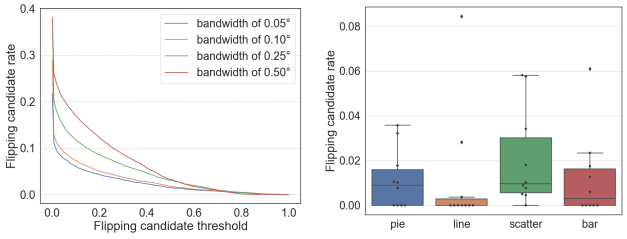

Figure 5: Left: flipping candidate rates for varying flipping candidate threshold and KDE Gaussian bandwidths. Larger thresholds lead to fewer fixations being classified as flipping candidates. Right: Descriptive statistics (boxplots and data items) of flipping candidate rates across different types of visualizations. A flipping candidate threshold of 0.5 was used.

3.1.2 Result. We use a 0.5° calibration error as the criterion to separate gaze data into two groups: low calibration error and high calibration error groups. We apply 0.05° KDE Gaussian bandwidth to the low calibration error group, and 0.25° to the high calibration error group. Figure 5 (left) illustrates how the FCR behaves under different flipping candidate thresholds. Larger thresholds lead to fewer fixations being classified as flipping candidates. Figure 5 (right) illustrates descriptive statistics of flipping candidate rates across different types of visualisations under a flipping candidate threshold of 0.5. The FCR of *scatter plots* are the highest, and *line plots* are the smallest among visualisation types. Figure 6 illustrates the occurrences of different AOIs involved in rank 2 flipping candidates in each visualisation type. In *line*, *bar*, and *scatter plots*, TS (Title, Source etc.) takes a majority of flipping candidates, ranking first place in *line* and *bar*, and second place in *scatter plots*. Figure 7 shows the Sequence Score between the original and flipped scanpaths across visualisation types under flipping candidate threshold 0.2. Participants are separated into two groups based on calibration error. We use a 0.5° calibration error as the criterion to separate gaze data into two groups: low calibration error and high calibration error groups. We apply 0.05° KDE Gaussian bandwidth to the low calibration error group, and 0.25° to the high calibration error group. We observed a significant difference in *line plots* and *pie plots* across low and high calibration error groups (post hoc t-test: *line*: $t(165) = 2.43$, $p = 0.016$, *pie*: $t(161) = 2.51$, $p = 0.013$), but the difference cannot be confirmed for *bar plots* ($t(159) = 0.54$, $p = 0.588$) or *scatter plots* ($t(156) = 1.38$, $p = 0.172$).

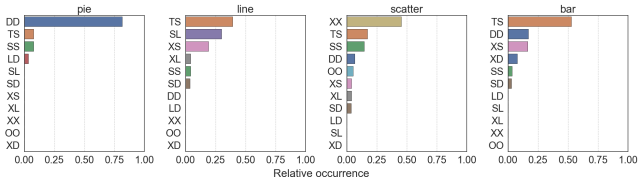

Figure 6: Analysis of the AOIs involved in flipping candidates of rank 2. Each AOI pair corresponds to a fixation covering those two individual AOIs. A flipping candidate threshold of 0.5 is used. AOI label taxonomy is adopted from [Borkin et al. 2015]. A: Annotation, D: Data, G: Graphics, L: Legend, O: Object, S: Source, paragraph, label, and header row text, denoted as Source etc., T: Title, X: Axis.

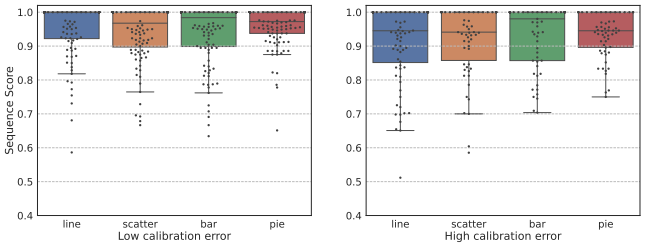

Figure 7: Sequence Score between the original and flipped scanpaths across visualisation types with a flipping candidate threshold of 0.2. All flipping candidates are flipped to the second probable AOI label.

3.2 Fixations Hit Any AOI

In most public gaze datasets of information visualisations, the raw gaze data are not accessible [Borkin et al. 2015; Polatsek et al. 2018]. It means that the calibration error is unknown, and the analysis in Section 3.1 is not applicable. However, we still can assess the impact of gaze uncertainty, that is, by enlarging the size of all AOIs uniformly. Given that the AOIs in visualisations can be close to one another, a drift and error in the gaze data make fixations land outside AOIs, or even hit different AOIs. In this analysis, we gradually enlarge the size of the AOI annotation to account for slight drifts in the gaze estimates.

3.2.1 Metrics. Since human attention is not naturally drawn by low saliency regions such as white spaces [Matzen et al. 2017], if there are too many fixations that land on empty or white spaces (in our case parts of a visualisation without any annotation), it is likely

indicative of large gaze estimation error. Hence, we propose Hit Any AOI Rate (HAAR), which is defined as the HAAR = $\frac{HIT}{HIT+OFF}$, where *HIT* represents the number of fixations that hit at least one AOI, and *OFF* represents the number of fixations that are not within any AOI.

3.2.2 Result. Fixations in this section are all adapted from the default fixation detection algorithm integrated in the EyeLink 1000 Plus eye tracker. Figure 8 demonstrates that *pie plots* have the highest HAAR among visualisation types without any enlargement. When the enlargement factor is larger than 0.2°, *bar plots* have the highest HAAR among visualisation types.

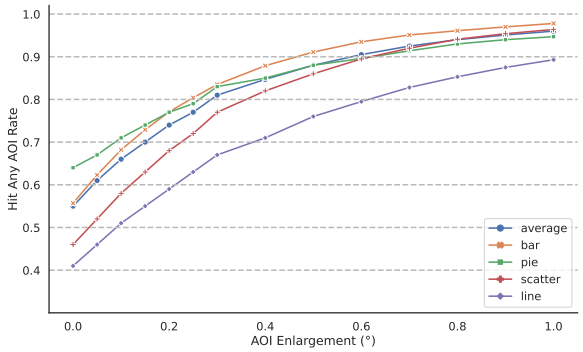

Figure 8: AOI enlargement factor by visual angle and the Hit Any AOI Rate (HAAR). When the AOI enlargement factor is larger than 0.2°, HAAR of bar plots exceeds pie plots to become the highest.

4 DISCUSSION

In this work, we demonstrated that gaze uncertainty can significantly impact subsequent AOI-based analysis such as scanpaths, including comparisons of scanpaths using similarity metrics. Using the two proposed metrics, the Flipping Candidate Rate (FCR) and Hit Any AOI Rate (HAAR), we identified several interesting findings that we discuss below.

Flipping candidate threshold and AOI enlargement factor. Since there is no AOI ground truth for gaze data, i.e., which AOI the participants really look at, it is difficult to identify whether fixations are assigned to the correct AOI. Hence, there is no deterministic rule to set the flipping candidate threshold and AOI enlargement factor. Figure 5 shows that the flipping candidate rate varies between 0.01 to 0.40 as the threshold changes, so a proper threshold becomes crucial for later analysis. Figure 8 illustrates the HAAR under different values of the AOI enlargement factor. A 1.0° AOI enlargement makes the HAAR increase from below 70 % to above 80 % for all kinds of visualisation types. This shows that AOI enlargement is an effective strategy to compensate for the influence of gaze estimation error, especially when only fixations are available [Borkin et al. 2015]. This is also a bio-plausible strategy since humans can perceive visual information in the foveal region [Jonas et al. 2015].

Guidelines on parameter selection. Here, we give a general guideline about how to choose a proper flipping candidate threshold and an AOI enlargement factor. When AOIs are so close to one another that the gaze estimation error cannot be ignored, a smaller flipping candidate threshold (e.g. 0.2) and a larger enlargement factor (e.g. 0.8°) are desired. A smaller flipping candidate threshold ensures that more ambiguous fixations can be detected, and a larger enlargement factor compensates more for the gaze estimation error to correct slight shifts or drifts of the gaze data. However, enlarging the size of an AOI too much will lead to overlapping AOIs, which then points to an increase in the flipping candidate rate.

Gaze uncertainty across visualisation types. Figure 5 shows that *line* and *pie plots* have fewer flipping candidates than *bar* and *scatter plots*. Moreover, in Figure 7, the sequence scores of *line* and *pie plots* between low and high calibration error groups is significant. This indicates that the impact of gaze uncertainty on *bar* and *scatter plots* was more severe than *line* and *pie plots* on MASSVIS dataset [Borkin et al. 2013]. While it is unclear whether such differences between visualisation types also hold on different datasets or visualistion designs, it opens up an opportunity for future research. Future work should investigate methods to design and optimise, e.g. different parameters for *bar* and *scatter plots*, to make them more robust against gaze uncertainity and limit such effects on any subsequent analysis. Figure 4 gives an impression of how different thresholds influence the flipping candidates in each visualisation type. The extent to which flipping candidates may threaten the validity of later analysis stages depends on the actual AOIs it overlays. A flipping candidate that overlays AOIs that share the same labels will not cause a difference in later analysis stages. As shown in Figure 6, the majority of flipping candidates occurring in *scatter* and *pie plots* can be considered insignificant, such as XX (Axis), SS (Source etc.), and DD (Data). Moreover, there are flipping candidates that overlay semantically different AOIs, such as TS (Title, Source etc.), SL (Source etc., Legend), and XD (Axis, Data). For example, in Figure 4, the *bar plots* shows two fixations that overlay an axis and a data item, while the red fixation in the *pie plots* is an example of SL.

5 CONCLUSION

This paper demonstrated and assessed the impact of gaze uncertainty on AOIs in information visualisations by introducing two effective metrics: Flipping Candidate Rate (FCR) and Hit Any AOI Rate (HAAR). Results showed that gaze uncertainty is a key factor that may impact the credibility of eye tracking studies and any resulting findings. While this paper addresses information visualisations, it also has a strong potential as an extension to other visualisation fields, such as volume visualisation or scientific visualisation in general.

ACKNOWLEDGMENTS

Y. Wang, M. Koch, and D. Weiskopf were funded by the Deutsche Forschungsgemeinschaft (DFG, German Research Foundation) - Project-ID 251654672 - TRR 161. M. Bâce was funded by a Swiss National Science Foundation (SNSF) Early Postdoc. Mobility Fellowship (grant number 199991). A. Bulling was funded by the European Research Council (ERC; grant agreement 801708).

We would like to thank reviewers for their insightful comments, Constantin Ruhdorfer for the gaze data processing toolbox, Nuo

Chen for eye-tracking data collection, Dominike Thomas for paper editing support, as well as Guanhua Zhang and Sruthi Radhakrishnan for helpful comments on this paper.

REFERENCES

Michael Barz, Florian Daiber, and Andreas Bulling. 2016. Prediction of gaze estimation error for error-aware gaze-based interfaces. In *Proceedings of the ACM Symposium on Eye Tracking Research & Applications*. 275–278.

Michael Barz, Florian Daiber, Daniel Sonntag, and Andreas Bulling. 2018. Error-aware gaze-based interfaces for robust mobile gaze interaction. In *Proceedings of the ACM Symposium on Eye Tracking Research & Applications*. 1–10.

Tanja Blascheck, Kuno Kurzhals, Michael Raschke, Michael Burch, Daniel Weiskopf, and Thomas Ertl. 2017. Visualization of eye tracking data: A taxonomy and survey. *Computer Graphics Forum* 36, 8 (2017), 260–284.

Michelle A Borkin, Zoya Bylinskii, Nam Wook Kim, Constance May Bainbridge, Chelsea S Yeh, Daniel Borkin, Hanspeter Pfister, and Aude Oliva. 2015. Beyond memorability: Visualization recognition and recall. *IEEE Transactions on Visualization and Computer Graphics* 22, 1 (2015), 519–528.

Michelle A Borkin, Azalea A Vo, Zoya Bylinskii, Phillip Isola, Shashank Sunkavalli, Aude Oliva, and Hanspeter Pfister. 2013. What makes a visualization memorable? *IEEE Transactions on Visualization and Computer Graphics* 19, 12 (2013), 2306–2315.

Michael Burch, Lewis Chuang, Brian Fisher, Albrecht Schmidt, and Daniel Weiskopf. 2017. *Eye Tracking and Visualization: Foundations, Techniques, and Applications. ETVIS 2015.* Springer.

Gautier Drusch, JC Bastien, and Stéfane Paris. 2014. Analysing eye-tracking data: From scanpaths and heatmaps to the dynamic visualisation of areas of interest. *Advances in Science, Technology, Higher Education and Society in the Conceptual Age: STHESCA* 20, 205 (2014), 25.

Benedikt V Ehinger, Katharina Groß, Inga Ibs, and Peter König. 2019. A new comprehensive eye-tracking test battery concurrently evaluating the Pupil Labs glasses and the EyeLink 1000. *PeerJ* 7 (2019), e7086.

Anna Maria Feit, Shane Williams, Arturo Toledo, Ann Paradiso, Harish Kulkarni, Shaun Kane, and Meredith Ringel Morris. 2017. Toward everyday gaze input: Accuracy and precision of eye tracking and implications for design. In *Proceedings of the 2017 CHI Conference on Human Factors in Computing Systems*. 1118–1130.

Joseph H. Goldberg and Jonathan I. Helfman. 2010. Comparing information graphics: A critical look at eye tracking. In *Proceedings of the 3rd BELIV'10 Workshop: BEyond Time and Errors: Novel EvaLuation Methods for Information Visualization*. 71–78.

Rahul A Jonas, Ya Xing Wang, Hua Yang, Jian Jun Li, Liang Xu, Songhomitra Panda-Jonas, and Jost B Jonas. 2015. Optic disc-fovea angle: the Beijing Eye Study 2011. *PLoS One* 10, 11 (2015), e0141771.

Laura E Matzen, Michael J Haass, Kristin M Divis, Zhiyuan Wang, and Andrew T Wilson. 2017. Data visualization saliency model: A tool for evaluating abstract data visualizations. *IEEE Transactions on Visualization and Computer Graphics* 24, 1 (2017), 563–573.

Jacob L Orquin, Nathaniel JS Ashby, and Alasdair DF Clarke. 2016. Areas of interest as a signal detection problem in behavioral eye-tracking research. *Journal of Behavioral Decision Making* 29, 2-3 (2016), 103–115.

Jacob L Orquin and Kenneth Holmqvist. 2018. Threats to the validity of eye-movement research in psychology. *Behavior Research Methods* 50, 4 (2018), 1645–1656.

Alex Pang, Craig M. Wittenbrink, and Suresh K. Lodha. 1997. Approaches to uncertainty visualization. *The Visual Computer* 13, 8 (1997), 370–390.

Patrik Polatsek, Manuela Waldner, Ivan Viola, Peter Kapec, and Wanda Benesova. 2018. Exploring visual attention and saliency modeling for task-based visual analysis. *Computers & Graphics* 72 (2018), 26–38.

Keith Rayner. 1998. Eye movements in reading and information processing: 20 years of research. *Psychological Bulletin* 124, 3 (1998), 372.

Hosnieh Sattar, Andreas Bulling, and Mario Fritz. 2017. Predicting the category and attributes of visual search targets using deep gaze pooling. In *Proceedings of the IEEE International Conference on Computer Vision Workshops (ICCVW)*. 2740–2748.

Christoph Schulz, Michael Burch, Fabian Beck, and Daniel Weiskopf. 2015. Visual data cleansing of low-level eye-tracking data. In *Workshop on Eye Tracking and Visualization*. Springer, 199–216.

Meredith M. Skeels, Bongshin Lee, Greg Smith, and George G. Robertson. 2010. Revealing uncertainty for information visualization. *Information Visualization* 9, 1 (2010), 70–81.

Yao Wang, Chuhan Jiao, Mihai Bâce, and Andreas Bulling. 2021. VisRecall: Quantifying information visualisation recallability via question answering. *arXiv preprint arXiv:2112.15217* (2021).

Daniel Weiskopf. 2022. Uncertainty visualization: Concepts, methods, and applications in biological data visualization. *Frontiers in Bioinformatics* 2 (2022).

Yaqi Xie, Hao Wang, Chaoquan Luo, Zhuo Yang, and Yinwei Zhan. 2021. GazeMetro: A Gaze-Based Interactive System for Metro Map. In *The 23rd International ACM SIGACCESS Conference on Computers and Accessibility*. 1–3.

Zhibo Yang, Lihan Huang, Yupei Chen, Zijun Wei, Seoyoung Ahn, Gregory Zelinsky, Dimitris Samaras, and Minh Hoai. 2020. Predicting goal-directed human attention using inverse reinforcement learning. In *Proceedings of the IEEE/CVF Conference on Computer Vision and Pattern Recognition*. 193–202.

Kiwon Yun, Yifan Peng, Dimitris Samaras, Gregory J Zelinsky, and Tamara L Berg. 2013. Exploring the role of gaze behavior and object detection in scene understanding. *Frontiers in Psychology* 4 (2013), 917.

Yunfeng Zhang and Anthony J Hornof. 2014. Easy post-hoc spatial recalibration of eye tracking data. In *Proceedings of the ACM Symposium on Eye Tracking Research & Applications*. 95–98.